SECURE WATERMARKING TECHNIQUE FOR MEDICAL IMAGES WITH VISUAL EVALUATION

Majdi Al-qdah

Department of Computer Engineering, University of Tabuk, Tabuk, KSA

ABSTRACT

This paper presents a hybrid watermarking technique for medical images. The method uses a combination of three transforms: Discrete Wavelet Transform (DWT), Discrete Cosine Transform (DCT), and singular value decomposition (SVD). Then, the paper discusses the results of applying the combined method on different medical images from eight patients. The images were watermarked with a small watermark image representing the patients' medical data. The visual quality of the watermarked images (before and after attacks) was analyzed using five quality metrics: PSNR, WSNR, PSNR-HVS-M, PSNR-HVS, and MSSIM. The first four metrics' average values of the watermarked medical images before attacks were approximately 32 db, 35 db, 42 db, and 40 db respectively; while the MSSM index indicated a similarity between the original and watermarked images of more than 97%. However, the metric values decreased significantly after attacking the images with various operations even though the watermark image could be retrieved after almost all attacks. In brief, the initial results indicate that watermarking medical images with patients' data does not significantly affect their visual quality and they can still be used by medical staff.

KEYWORDS

Transforms, Watermarking, medical images, visual metrics

1. INTRODUCTION

Data hiding has increasingly become an important tool in authentication of images and protection of rightful owners copyright. Also, there is an increasing need to store and transfer patients' medical images over the Internet and other computer networks for sharing among medical staff in medical institutions all over the world. Image watermarking techniques that hides important details inside cover images can be divided into two broad domains: spatial domain and frequency domain [1, 2]. Various medical images based watermarking schemes have been proposed in literature [3,4,5]. Three of the most important frequency watermarking methods are the discrete cosine transform (DCT), discrete wavelet transform (DWT) and Singular Value Decomposition (SVD). Many researchers have used a hybrid of two or more transforms in order to compensate for the shortcomings of various transforms.

There are many examples of spatial domain techniques such as LSB substitution, spread spectrum, and patchwork. Lin et al. [6] proposed a spatial watermarking methods where the watermark logo is fused with noise bits first, and then XORed with the feature value of the image by 1/T rate forward error correction (FEC), where T is the times of data redundancy. The watermark bits are extracted by majority voting.

Rosiyadi et al.[7] proposed a robust hybrid watermarking method based on DCT and SVD. The DCT is applied on the host image using the zigzag space-filling curve (SFC) for the DCT coefficients and then the SVD is applied on the DCT coefficients. Horng et al. [8] proposed a

DOI : 10.5121/sipij.2018.9101

robust adaptive watermarking method based on DCT, SVD and Genetic Algorithm (GA). The host image luminance masking is used and the mask of each sub-band area is transformed into frequency domain. Subsequently, the watermark image is embedded by modifying the singular values of DCT-transformed host image with singular values of mask coefficients of host image and the control parameter of DCT-transformed watermark image using GA. Singh et al. [9] proposed a robust hybrid watermarking technique using DWT, DCT, and SVD. First, the host image into first decomposed by DWT and the Low frequency band (LL) and watermark image are transformed using DCT and SVD. Then the S vector of watermark image is embedded in the S component of the host image and the watermarked image is generated by inverse SVD on modified S vector and original U, V vectors followed by inverse DCT and inverse DWT.

2. METHODOLOGY

The following sections will give details of the used watermarking algorithm and evaluation metrics.

2.1. Watermarking algorithms

The designed and implemented algorithm is a combination of three frequency domain techniques: discrete wavelet transform (DWT), discrete cosine transform (DCT), and singular value decomposition (SVD). DWT decomposes an image into frequency channels of constant bandwidth on a logarithmic scale by separating an image into a set of four non-overlapping multi-resolution sub bands denoted as lower resolution approximation image (LL), horizontal (HL), vertical (LH) and diagonal (HH) with the availability of multiple scale wavelet decomposition. The watermark is usually embedded into the high frequency detail sub-bands (HL, LH and HH sub-band) because the human visual system (HVS) is sensitive to the low-frequency LL part of the image. We can usually embed sensitive data such as medical information in higher level sub-bands since the detail levels carry most of the energy of the image [10]. DWT achieves higher robustness since it has the characteristics of space frequency localization, multi-resolution representation, multi-scale analysis, adaptability and linear complexity [11].

Also, DCT has a very good energy compaction property. It separates the image into different low, high, and middle frequency coefficients [12]. The watermark is embedded in the middle frequency band that gives additional resistance to the lossy compression techniques with less modification of the cover image. The DCT coefficients D(i, j) matrix of an image (N x M) with pixel intensity I(x, y) are obtained as follows:

$$D(i,j) = \frac{1}{\sqrt{2N}} C(i)C(j) \sum_{x=0}^{N-1} \sum_{y=0}^{M-1} I(x,y) \cos\left(\frac{(2x+1)i\pi}{2N}\right) \cos\left(\frac{(2y+1)i\pi}{2M}\right) \quad \text{(Eq.1)}$$

$$C(i), C(j) = \frac{1}{\sqrt{N}}, \frac{1}{\sqrt{M}} \text{ for } i,j = 0 \text{ and } C(i), C(j) = \sqrt{\frac{2}{N}}, \sqrt{\frac{2}{M}} \text{ for } i,j = 1,2, \ldots \ldots N-1 \text{ or } M-1 \quad \text{(Eq.2)}$$

SVD of a rectangular matrix R_m is a decomposition of the form

$$R_m = USV^T \quad \text{(Eq.3)}$$

Where R_m is a M x N matrix, U and V are orthonormal matrices, and S is a diagonal matrix comprised of singular values of R_m. The singular values $S_1 \geq S_2 \geq S_3 \geq \ldots\ldots S_{n-1} \geq S_n \geq 0$ are unique values that appear in descending order along the main diagonal of S. They are obtained by taking the square root of the Eigen values of $R_m R_m^T$ and $R_m^T R_m$. The U, V are not unique. In the Singular Value Decomposition, the slight variations of singular values do not affect the visual

perception of the cover image, which achieves better quality of the watermarked image and better robustness against attacks. Also, singular values represent the intrinsic algebraic image properties [12].

Figure 1 shows the approach taken in embedding the patients' data into a cover medical image; First, DCT is applied on the LL component of the DWT transformed cover image; SVD is applied to the DCT coefficients. Then, the watermark is DCT transformed and the singular values of the SVD transformed coefficients are embedded in the singular values of the DWT transformed coefficients of the cover image. Figure 2 shows the extraction approach of the patient's image data from the watermarked image. The watermarked images is DWT and DCT transformed then SVD is applied to the DCT coefficients; the watermark is extracted from the LL sub band of DWT. For an added security, the watermark image can be encrypted before embedding it in the cover image.

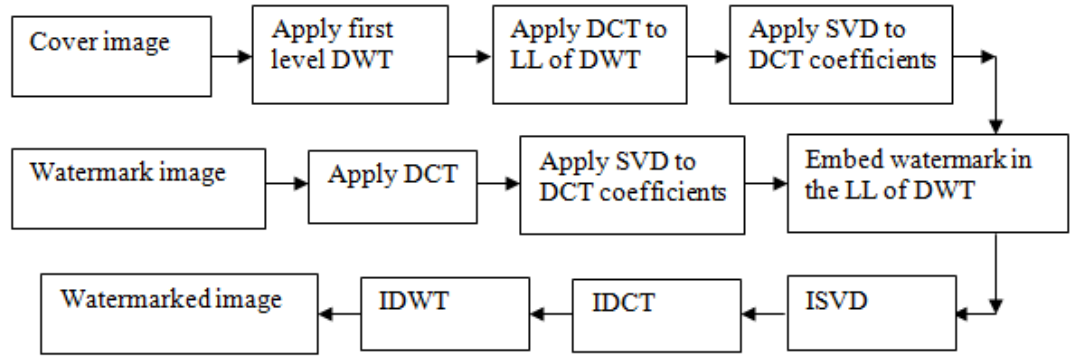

Figure1. Embedding process

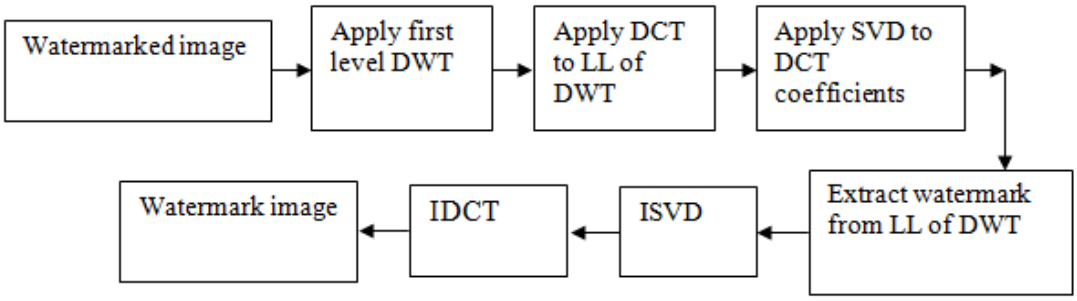

Figure 2. Extraction process

2.2. Evaluation metrics

Four visual metrics (WSNR, MSSIM, PSNR-HVS-M, and PSNR-HVS) described by Ponomarenko et. al. [13] are used for comparing the watermarked images with their originals. Traditionally, the efficiency of an image processing operation ; i.e. lossy compression is usually analyzed in terms of rate-distortion curves. These curves represent dependencies of PSNR (or MSE) on bits per pixel (bpp) or compression ratio (CR) where PSNR and MSE are calculated for some original image and the corresponding processed image.

$$PSNR = 10\log\left(\frac{255^2}{MSE}\right) \quad \text{(Eq.4)}$$

$$MSE = \sum_{i=1}^{N}\sum_{j=1}^{M}\frac{\left(I_{ij}^{d}-I_{ij}^{n}\right)^2}{NM} \quad \text{(Eq.5)}$$

where I_{ij}^{d}, I_{ij}^{n} denote the values of the original and processed pixels and N, M denote an image size [14]. In order to obtain a high imperceptibility of the watermarked image, it is desirable to have a high value of PSNR; meaning a lesser value of MSE.

Also, usually the similarity and differences between an original image and a processed image is measured by the Normalized Correlation (NC). Its value is generally 0 to 1. Ideally it should be 1 but a value 0.7 or higher is usually acceptable [15].

$$NC = \sum_{i=1}^{X}\sum_{j=1}^{Y}(I_{ij}^{d} \times I_{ij}^{n}) / \sum_{i=1}^{X}\sum_{j=1}^{Y}(I_{ij}^{d})^{2} \quad \text{.....(Eq6) [16]}$$

where I_{ij}^{d}, I_{ij}^{n} denote the values of the original and processed pixels and X, Y denote an image size.

Two different distorted images with the same PSNR value with respect to the same original image may give significantly different visual impact. It is well known that conventional quality metrics, such as MSE, SNR and PSNR do not always correlate with image visual quality [17,18]. Therefore, the choice of a proper visual quality metric for analysis and comparisons is always problematic since the human visual system (HVS) is nonlinear and it is very sensitive to contrast changes and to noise [19]. Many studies have confirmed that the HVS is more sensitive to low frequency distortions rather than high frequency components. The best performance was achieved by the metrics PSNR-HVS-M, PSNR-HVS, and WSNR [14] especially if there is noise or the images are to be compressed. HVS-based models are the result of trade-off between computational feasibility and accuracy of the model. HVS-based models can be classified into two categories: neurobiological models and models based on the psychophysical properties of human vision. Psychophysical HVS-based models are implemented in a sequential process that includes luminance masking, colour perception analysis, frequency selection, and contrast sensitivity [19].

Recently, processing of images is done using perceptual image quality assessment methods, which attempt to simulate the functionality of the relevant early human visual system (HVS) components. These methods usually involve a pre-processing process that may include image alignment, point-wise nonlinear transform, low-pass filtering that simulates eye optics, and color space transformation, a channel decomposition process that transforms the image signals into different spatial frequency as well as orientation selective subbands, an error normalization process that weights the error signal in each subband by incorporating the variation of visual sensitivity in different subbands, and the variation of visual error sensitivity caused by intra- or inter-channel neighbouring transform coefficients, and an error pooling process that combines the error signals in different subbands into a single quality/distortion value [20].

PSNR-HVS takes into account the HVS properties such as sensitivity to contrast change and sensitivity to low frequency distortions; while the PSNR-HVSM takes into account the contrast sensitivity function (CSF). Similar to PSNR and MSE, the visual quality metrics PSNR-HVS and PSNR-HVSM can be determined:

$$PSNR - HVS = 10 \log \frac{255^{2}}{MSE_{nf}^{HVS}} \quad \text{..... (Eq.7)}$$

$$MSE_{nf}^{HVS} = K \sum_{i=1}^{I-7}\sum_{j=1}^{J-7}\sum_{m=1}^{8}\sum_{n=1}^{8}((X[m,n]_{i,j} - X[m,n]_{ij}^{e})T_{c}[m,n]) \quad \text{..... (Eq.8)[21]}$$

where I,J denote image size, K=1 [(I-7)(J-7)64] , $X[m,n]_{i,j}$ are DCT coefficients of 8x8 image block for which the coordinates of its left upper corner are equal to i and j, Xij e are the DCT coefficients of the corresponding block in the original image, and $T_{c}[m,n]$ is the matrix of correcting factors [21].

The Weighted Signal to Noise Ratio (WSNR) is a noise metric where the difference (residual) between the original and the processed images must be noise. (WSNR) uses a Contrast Sensitivity Function (CSF) given by the following:

$$CSF = 2.6(0.02 + 0.1f_a)e^{-(0.1f_a)^{1.1}} \quad \text{(Eq.9)}$$

where f_a is a radial angular frequency

The WSNR between an original image (x) and a processed image (y) is:

$$WSNR = 10\log_{10}\left(\frac{\sum |CSF \times X(u,v)|^2}{\sum |CSF \times X(u,v) - Y(u,v)|^2}\right) \quad \text{(Eq.10)}$$

The structural similarity index (SSIM) measures the similarity between two images [19]. SSIM compares two images using information about luminous, contrast and structure. SSIM metric is calculated on various windows of an image. The measure between two windows x and y of common size N×N is given as follows:

$$SSIM(x,y) = \frac{\{(2u_x u_y + C_1)(2\sigma_{xy} + C_2)\}}{\{(u_x^2 + u_y^2 + C_1)(\sigma_x^2 + \sigma_y^2 + C_2)\}} \quad \text{(Eq.11)}$$

SSIM takes values between 1 and -1; u_x is an average of x, $u_y$is an average of y, σ_x, σ_y are the standard deviations between the original and watermarked image pixels; while C_1, C_2, are positive constant chosen to avoid the instability of SSIM measure.

MSSIM (Multi-Scale Structural Similarity) is a multi-scale extension of a SSIM metric. MSSIM [22] is introduced to incorporate the variations of viewing conditions to the previous single-scale SSIM measure. MSSIM is known as mean structural similarity index metric [22] and it is given by:

$$MSSIM(x,y) = \frac{1}{M}\sum_{i=1}^{M} SSIM(x_i, y_i) \quad \text{(Eq.12)}$$

where M is the correlation between two images x, y

Correlation is a similarity measure between two functions. The correlation measure between two functions x(x,y) and s(x,y) in discrete form is defined as:

$$M = \sum_{x=0}^{M-1}\sum_{y=0}^{N-1} r(x,y)[s(x,y)]^* \quad \text{(Eq.13)}$$

Where $[]^*$ is the complex conjugate, x=0, 1,…….., M-1 and y=0, 1,……, N-1

3. RESULTS

Figure 3 shows the eight medical cover images of size [512×512] and the patients' data watermark image of size [256×256] selected for the experiment. The medical images contain medical information based on the characteristics of each image and the purpose of its capture. The medical images reveal characteristics of the bones, tissues, vessels, nerves....etc. For example, the finger print image shows the shape and size of the prints while the ultrasound image shows the size and shape of the fetes. Thus, embedding a watermark image inside a medical cover image should preserve the existing medical information in the cover medical image: the unique pattern of the fingerprint, vessels and optical nerves inside the retina, bone fracture in the wrist, size and development signs of the fetus, shape, the position of the torn ligament, and sliced layers and soft tissue of the human skull. The patients' personal details can be embedded in the captured medical image in textual or image format and saved in one file. The patients' personal details (watermark) are embedded by the earlier discussed combined method of DWT, DCT, and SVD transforms; while the imperceptivity of the watermarked images is evaluated using PSNR, P-HVS, P-HVS-M, WSNR, and MSSIM. The metrics measure the imperceptivity of the watermarked images, which

is an important factor in medical images watermarking. The experiment was run under MATLAB simulation software.

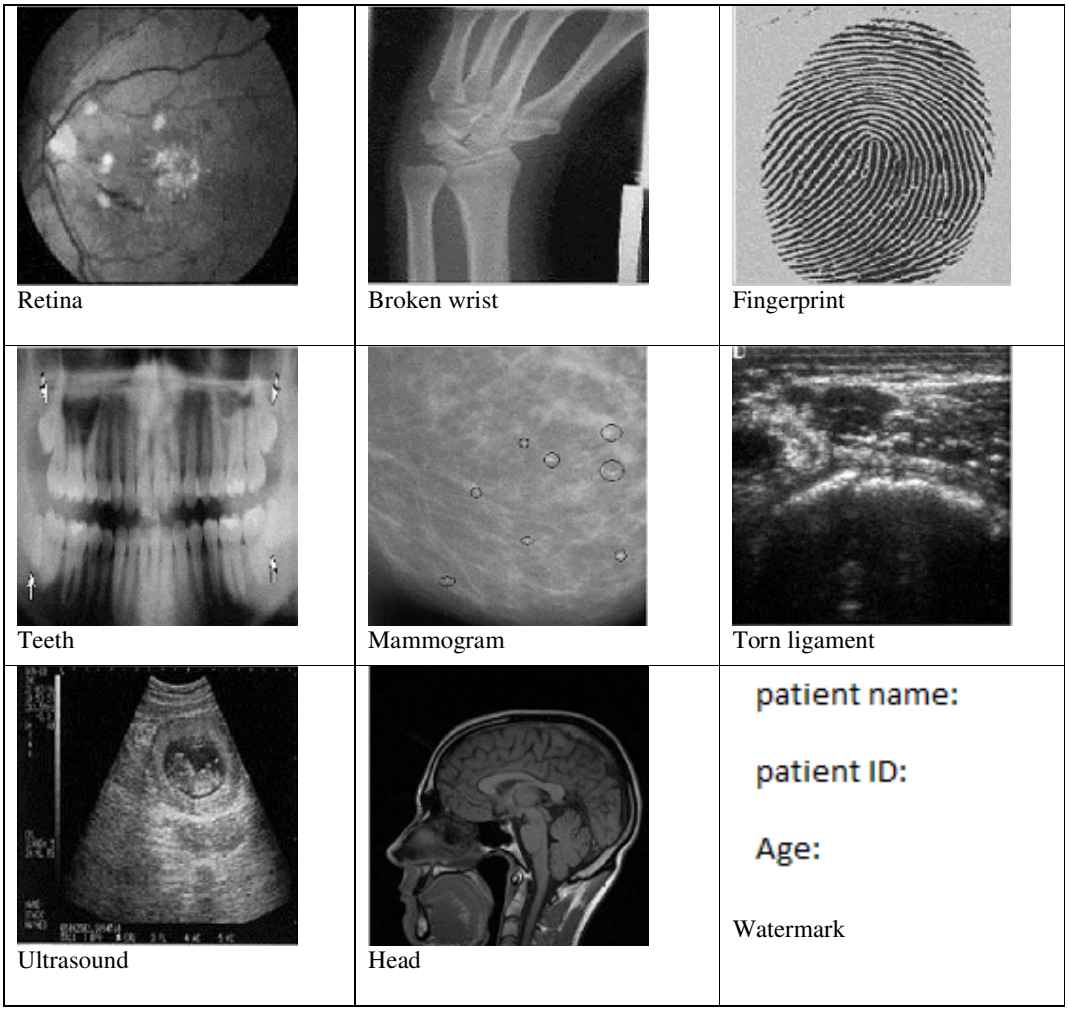

Figure 3. Eight cover images and one watermark

The algorithm was evaluated using five quality metrics. Table 1 shows the PSNR, P-HVS, P-HVS-M, WSNR, and MSSIM metrics among all the watermarked images before any attacks. It can be observed that the PSNR average value is about 32 db, P-HVS average value is around 35 db, P-HVS-M average value is about 42 db, and the WSNR average value varies from 35 db to 47 db. The MSSIM metric shows that the watermarked images are highly visually similar to the original images with similarity index values between the original and the watermarked images of more than 0.97%. Also, it can be observed that there is no significant difference between the average metric values among the various images; only the WSNR value of the of the Head image varies from one image to another with approximately 15 db difference between the Fingerprints image and the Head image; that is mainly due to the characteristics of the two images.

Table 1. Metric values of the watermarked images with watermark "Copyright"- not attacked

Image	PSNR	P-HVS	P-HVS-M	WSNR	MSSIM
Fingerprints	32.7049	34.8745	46.2079	47.0602	0.9920
Retina	32.9101	34.8738	40.4924	38.0317	0.9740
Torn Ligament	32.9784	34.8868	42.2467	39.5283	0.9846
Broken Wrist	32.7310	34.9020	40.7815	43.3029	0.9734
Teeth structure	32.7048	34.8898	41.4563	45.4571	0.9793
Ultrasound	33.2059	34.8428	41.3834	37.8052	0.9850
Head	33.3870	35.1103	40.0242	34.3916	0.9770
Mammogram	32.6940	34.8750	41.1925	46.0111	0.9738

To test the robustness, the watermarked image were attacked with various types of attacks. Tables 2 shows the average values of the same metrics for each image after the watermarked images are attacked with various operations (Gaussian noise, Salt & Pepper noise, 2D FIR filter, Cropping, Rotation & Cropping, Weiner filter, Intensity adjustment, Gaussian filter, and Sharpening).). It is observed that the numerical values decrease after an attack operation is performed on the images. Thus, there is a degradation in the quality of the attacked images. The drop in the numerical values is not significant after the Gaussian Noise, Salt & Pepper Noise, and 2D FIR filter attacks. The PSNR and other HVS metric values are similar among all watermarked images before and after attacks. The values of PSNR, P-HVS, P-HVS-M, and WSNR stay above the value of 20 db and the MSSIM metric values remain above 0.82%. On the other hand, there is a significant decrease in the values after the Cropping, Rotation & Cropping, Weiner Filter, Intensity adjustment, Gaussian filter, and Sharpening image attack operations. The numerical values of PSNR, P-HVS, P-HVS-M, and WSNR drop to less than 6 db while the MSSIM similarity index drops to 10% approximately. The watermark images can be clearly recovered after the Gaussian noise, Salt & Pepper noise, Intensity adjustment, Gaussian filter, and Sharpening attacks; but the recovered watermarks are distorted after the 2D FIR filter, Rotation & Cropping, and Weiner filter attacks. Even though the images are apparently distinguishable after those attacks the metric values drop significantly. Finally, there is no correlation between the drop in the metric values and the recovery of the watermark; for example, the P-HVS, P-HVS-M, and the WSNR values drop greatly after the sharpening attack but the watermark is fully recovered.

Table 2. Average metric values of all eight watermarked images after some attacks

Attack	PSNR	P-HVS	P-HVS-M	WSNR	MSSIM
No attack	32.9878	34.9307	41.7779	40.1183	0.9803
Gaussian Noise	19.9203	19.9790	22.6201	27.0916	0.8212
Salt & Pepper Noise	24.6345	24.8935	27.9674	32.1470	0.9304
2D FIR filter	25.3646	26.6690	30.0951	35.1960	0.9618
Cropping	13.7111	9.5336	9.5670	8.1109	0.7391
Rotation & Cropping	5.9136	1.7664	1.7862	0.2728	0.0982
Weiner Filter	5.9212	1.7732	1.7950	0.2801	0.1029
Intensity adjustment	5.9431	1.7932	1.8150	0.3004	0.1113
Gaussian filter	5.9212	1.7743	1.7950	0.2802	0.1030
Sharpening	5.9214	1.7733	1.7951	0.2801	0.1031

The limitation of this research is that the algorithms cannot determine how much of medical information is lost after watermarking medical images or even after attacking the images. Only medical doctors can decide the important segments of a medical image that are affected by watermarking or by attacking. Also, the effects can vary from one image to another. Finally, recovering the watermark after some attacks does not necessarily indicate that all medical information is preserved.

4. CONCLUSIONS

The results of this limited research show that watermarking medical images with a watermark of patients' personal details does not significantly affect the visual quality of the original medical images; and they can be utilized for their medical purpose. It was experimentally quantitatively demonstrated using Human Visual System (HVS) metrics that the watermarked medical images were similar to their originals. Also, choosing the appropriate watermarking algorithm is essential to obtain the robustness, imperceptivity and security needed to protect the patients' personal data inside a medical image and there are many transform domain algorithms that are available and can be utilized to preserve the characteristics of the original images. Artificial intelligence methods will be used in the future to classify the effectiveness of new algorithms.

ACKNOWLEDGEMENTS

The authors would like to acknowledge financial support of this work from the Deanship of Scientific Research (DSR), University of Tabuk, Tabuk, Saudi Arabia, under grant no. S/0180/1438

REFERENCES

[1] Lee, S.hyun. & Kim Mi Na, (2008) “This is my paper”, ABC Transactions on ECE, Vol. 10, No. 5, pp120-122.

[2] Gizem, Aksahya & Ayese, Ozcan (2009) Coomunications & Networks, Network Books, ABC Publishers.

[3] Ashourian (2006), A new mixed spatial domain watermarking of three dimensional triangle mesh, proceeding of the 4th international conference on computer graphics and interactive techniques in Australia and Southeast Asia

[4] Ahmed (2008), Intelligent watermark recovery using spatial domain extension, International conference on intelligent information hiding and multimedia signal processing, IIHMSP' 08

[5] Lai, C.C., Tsai, C.C. (2010): Digital Image Watermarking Using Discrete Wavelet Transform and Singular Value Decomposition. IEEE Transactions on Instrumentation and Measurement 59(11), 3060-3063

[6] Soliman MM, Hassanien AE, Ghali NI, Onsi HM, (2012) "An Adaptive Watermarking Approach for Medical Imaging using Swarm Intelligence", Int Journal Smart Home 6:37-50

[7] Zain J, Clarke M, (2011) Security in Telemedicine: Issue in Watermarking Medical Images, International Conference: Science of Electronic, Technologies of Information and Telecommunications

[8] Lin W-H, Horng S-J, Kao T-W, Chen R-J, Chen Y-H, Lee C-L, Terano T (2009) Image copyright protection with forward error correction. Expert Syst Appl 36(9):11888–11894

[9] Rosiyadi D, Horng S-J, Fan P, Wang X (2012) Copyright protection for e-government document images. IEEE MultiMedia 19(3):62–73

[10] Shi-Jinn H, Rosiyadi D, Fan P, Wang X, Khan MK (2014) An adaptive watermarking scheme for e-government document images. Multimed Tools Appl 72(3):3085

[11] Singh AK, Dave M, Mohan A (2014) Hybrid technique for robust and imperceptible image watermarking in DWT- DCT-SVD domain. Natl Acad Sci Lett 37(4):351–358

[12] Giakoumaki A, Pavlopoulos S, KoutsourisD (2006) Secure and efficient health data management through multiple watermarking on medical images. Med Biol Eng Comput 44:619–631

[13] Lin W-H, Wang Y-R, Horng S-J, Kao T-W, Pan Y (2009) A blind watermarking method using maximum wavelet coefficient quantization. Expert Syst Appl 36(9):11509–11516

[14] Liu, R., Tan, T. (2002): An SVD-based watermarking scheme for protecting rightful ownership, IEEE Transactions on Multimedia 4(1), 121-128

[15] N. Ponomarenko, V. Lukin, M. Zriakhov, K. Egiazarian, and J. Astola (2006), Estimation of accessible quality in noise image compression, in Proceedings of European Signal Processing Conference (EUSIPCO '06), pp. 1–4, Florence, Italy.

[16] S. G. Chang, B. Yu, and M. Vetterli, (2000) Adaptive wavelet thresholding for image denoising and compression, IEEE Transactions on Image Processing, vol. 9, no. 9, pp. 1532–1546.

[17] Shaick (2000), A hybrid transform method for image denoising. 10th European. Signal Processing Conference,

[18] Z. Wang and A. C. Bovik (2006). Modern Image Quality Assessment. Morgan and Claypool Publishing Company, New York

[19] Z. Wang, A. C. Bovik, H. R. Sheikh (2004), and E. P. Simoncelli, "Image quality assessment: from error visibility to structural similarity," IEEE Transactions on Image Processing, vol. 13, no. 4, pp. 600–612

[20] Z. Wang and A. C. Bovik (2009), Mean squared error: love it or leave it? A new look at signal fidelity measures, IEEE Signal Processing Magazine, vol. 26, no. 1, pp. 98–117.

[21] N. Ponomarenko, F. Battisti, K. Egiazarian, J. Astola, and V. Lukin (2009), Metrics performance comparison for color image database, in Proceedings of the 4th International Workshop on Video Processing and Quality Metrics, pp. 1–6, Scottsdale, Ariz, USA, CD-ROM.

[22] Zhou Wang1, Eero P. Simoncelli1 and Alan C (2003). Bovik multi-scale structural similarity for image quality assessment. Proceeding of the 37th IEEE Asilomar Conference on Signals, Systems, and Computers, Pacific Grove, CA, Nov. 9-12, 2003.

[23] N. Nill, (1985) A visual model weighted cosine transform for image compression and quality assessment, IEEE Transactions on Communications COM-33, pp. 551-557.

[24] R. F. Zampolo, R. Seara, (2003) A Measure for Perceptual Image Quality Assessment", in Proc. of Int. Conf. on Image Proc., Barcelona, Spain, pp: 433-436, Sept.

AUTHOR

Dr. Majdi is currently an assistant professor in department of computer engineering at the University of Tabuk Saudi Arabia. His research interests include data hiding, cryptography, medical imaging, and other various other current engineering topics.